A LATTICE BOLTZMANN COUPLED TO FINITE VOLUMES METHOD FOR SOLVING PHASE CHANGE PROBLEMS

by

Mohammed El GANAOUI and El Alami SEMMA

Original sicientific paper
UDC: 536.242:517.95
BIBLID: 0354-9836, *13* (2009), 2, 205-216
DOI: 10.2298/TSCI090205E

A numerical scheme coupling lattice Boltzmann and finite volumes approaches has been developed and qualified for test cases of phase change problems. In this work, the coupled partial differential equations of momentum conservation equations are solved with a non uniform lattice Boltzmann method. The energy equation is discretized by using a finite volume method. Simulations show the ability of this developed hybrid method to model the effects of convection, and to predict transfers. Benchmarking is operated both for conductive and convective situation dominating solid/liquid transition. Comparisons are achieved with respect to available analytical solutions and experimental results.

Key words: *finite volumes, lattice Boltzmann, computational fluid dynamics, phase change, enthalpy method*

Introduction

Computational fluid dynamics (CFD) simulations of flows and transfers are generally based on space and temporal discretization of differential equations describing macroscopic state, *i. e*., solving continuum mechanics formulation for the conservation equations. However, their solutions can be very difficult when considering complex geometries and moving boundaries and/or with multi-physics state. This justifies the development of new routes of simulations such as lattice Boltzmann (LB) approaches. These methods are in progress and become a serious alternative to traditional CFD methods [1-4]. LB methods are especially well suited to simulate flows in complex geometries, and they are straightforwardly implemented on parallel machines [5-6]. The main goal of these methods is being to model the fluid flow at the microscopic level in term of local interactions between particles. Several advantages are listed for these methods. For instance, the method should be easier and allows an intuitive treatment of particular conditions like presence of obstacles [7]. However, classical methods still exhibiting indubitable advantages and the coupling with new approaches become an interesting way to be innovative for solving stiff problems.

The purpose of this paper is to develop an efficient and accurate numerical methodology to deal with solid/liquid phase change problems generally treated by using a combination of adequate partial differential equations formulation (multidomains, enthalpy, ...) and classical discretisation (finite volumes, finite elements, ...) [8]. The present scheme will take advantage both from the LB method and finite volume (FV) ones. A control volume numerical method based on high-order schemes will be used for energy equation. The LB method based on distribution functions is used to simulate fluid flows. The evolution equations for these distributions are de-

rived from the continuous Boltzmann equation with appropriate approximations for incompressible flows. The performance of the method (coupling LB to FV) is then examined for the restricted configuration to fluid flow followed by a comparison with the experimental results of Gau *et al.* [9] on the morphology and positions of the solid/liquid interface (this is a very popular test case for classical methods).

Models and solution methods

The solution based on continuum medium formulation

Classically, the balance equations are derived from continuum media theory to describe transfers of mass, momentum, and energy (and eventually species). Theses governing equations for natural convection with phase change can be written as:

$$\vec{u} \quad 0 \tag{1}$$

$$\frac{\partial \vec{u}}{\partial t} \quad (\vec{u} \quad)\vec{u} \qquad P \quad \mathrm{Pr} \quad {}^2\vec{u} \quad \mathrm{Ra}T \tag{2}$$

$$\frac{\partial T}{\partial t} \quad \vec{u} \quad (\quad T) \qquad {}^2T \quad \frac{1}{\mathrm{Ste}} \frac{\partial \phi}{\partial t} \tag{3}$$

where $\vec{u}$ is the velocity vector, T – the temperature, P – the pressure, and ϕ – the liquid fraction.

The grouping Pr, Ra, and Ste refers to Prandtl, Rayleigh, and Stefan numbers, respectively, which are non-dimensional numbers based on physical properties and commonly used in CFD:

$$\mathrm{Pr} \quad \frac{\nu}{\alpha}, \quad \mathrm{Ra} \quad \frac{g\beta \Delta T H^3}{\nu \alpha}, \quad \text{and} \quad \mathrm{Ste} \quad \frac{Cp\Delta T}{L_\mathrm{f}} \tag{4}$$

where ν and α are the kinetic viscosity and the thermal diffusivity, respectively.

With assuming constant properties (ν, α) and Boussinesq approximation for density ρ: $\rho = \rho_0[1 - \beta(T - T_0)]$, where ρ_0 and T_0 are the reference values of density and temperature, respectively, and β is the coefficient of thermal expansion.

Such conservative system of equation is completed by initial and boundary conditions (specified here for each application). Generally it is discretized by classical methods as finite differences, finite elements, or FV. In the following the FV is used for scalar equation (eq. 3) because the task of the present work is LB and FV coupling. LB method will be used for solving eqs. 1 and 2.

The LB method provides another way for solving the dynamic field. LB methods are a class of mesoscopic particle based approaches to simulate fluid flows. Historically, the LB approach is developed from lattice gases, although it can also be derived directly from the simplified Boltzmann BGK (Bhatangar-Gross-Krook) equation. In lattice gases, the particles jump from one lattice node to the next, according to their (discrete) velocity. This is called the propagation phase. Then, the particles collide and get a new velocity, the collision phase. Hence the simulation proceeds in an alternation between particle propagations and collisions. The two phases can be clearly distinguished.

The dynamic solution based on LB procedure

The LB method employed in this study uses a square lattice (Frisch-Hasslacher--Pomeau model) (fig. 1) [10], the main equation is:

$$f_i(\vec{x} \quad \vec{c}_i\delta t,\ t \quad \delta t) \quad f_i(\vec{x},t) \quad \Omega_i \tag{5}$$

where f_i is the particle distribution function defined for the finite set of discrete particle velocity vectors $\vec{c}_i$. The collision term Ω_i on the right hand side of eq. (5) uses the BGK approximation [11]. The essence of this approximation for LB method is that the collision term Ω_i will be replaced by the well-known single time relaxation approach:

$$\Omega_i \quad \frac{f_i \quad f_i^{eq}}{\tau} \quad F_i \tag{6}$$

where τ is the relaxation time and f_i^{eq} is the local equilibrium distribution function that has an appropriately prescribed functional dependence on the local hydrodynamic properties.

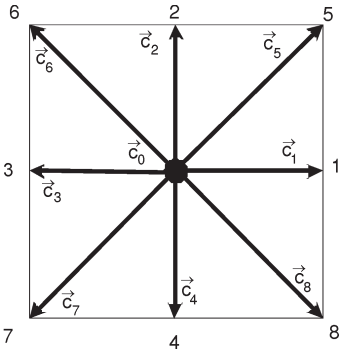

Figure 1. Schematic diagram of the D2Q9 lattice

F_i represents the external force fields that give rise to a body force. This force term is self-consistently generated by the neighbouring distribution functions around each lattice site and doesn't violate either the local mass conservation or the global momentum conservation. The total imposed body force is given by:

$$\sum_i \vec{e}_i F_i \quad \vec{F} \quad \rho\vec{G} \tag{7}$$

where $\vec{G}$ is the buoyancy source term which can be described as:

$$\vec{G} \quad \vec{g}\beta(T \quad T_{ref}) \tag{8}$$

This relation is consistent with the Boussinesq approximation. $\vec{g}$ represents the gravity acceleration, β is the volumetric thermal expansion coefficient, and T_{ref} – the reference temperature.

The present LB equation for dynamical system is completed by choosing the equilibrium distribution:

$$f_i^{eq} \quad \omega_i\rho\ 1 \quad 3\frac{\vec{c}_i \quad \vec{u}}{c^2} \quad \frac{9}{2}\frac{(\vec{c}_i \quad \vec{u})^2}{c^4} \quad \frac{3}{2}\frac{\vec{u} \quad \vec{u}}{c^4} \tag{9}$$

where ω_i are the weights that are given by the length of the velocity vector:

$$\omega_0 \quad 0 \quad \text{and} \quad \omega_{2k} \quad \frac{1}{36};\quad \omega_{2k\ 1} \quad \frac{1}{9} \quad \text{for} \quad k \quad 1,2,\ldots \tag{10}$$

The discrete velocities for D2Q9 lattice are defined as:

$$\vec{c}_0 \quad (0,0)$$
$$\vec{c}_{2k\ 1} \quad c\cos k\frac{\pi}{2}, \sin k\frac{\pi}{2} \quad \text{and} \quad \vec{c}_{2k} \quad \sqrt{2}c\cos(2k \quad 1)\frac{\pi}{4}, \sin(2k \quad 1)\frac{\pi}{4} \tag{11}$$

for $k = 1, 2, ...$, where $c = \delta x/\delta t$ and δx and δt are the lattice space step and the lattice time step size, respectively. The macroscopic variables such as density and velocity in non-dimensional form are obtained as:

$$\rho(\vec{x},t) \quad \sum_i f_i(\vec{x},t) \tag{12}$$

$$\rho\vec{u}(\vec{x},t) \quad \sum_i \vec{c}_i f_i(\vec{x},t) \tag{13}$$

The Chapman-Enskog expansion for the density distribution function can recover the continuity and Navier-Stokes equations. The detailed derivation of this procedure is given by Hou *et al*. [12] and will not be shown here. The kinematic viscosity ν is given by:

$$\nu \quad \tau_\nu \quad \frac{1}{2} \; c_s^2 \tag{14}$$

As explained, the LB are generally exploited in a uniform grid, but it is well known in CFD that problems can exhibits areas of high gradients of solution. For instance, for high Rayleigh number, the thermal boundary layer is very thin. In order to capture the physical properties within the boundary layer, a higher density of grid points is needed.

Implementation of LB method on non-uniform grid

This can be carried out by the non-uniform grid using Taylor series expansion and least square based lattice Boltzman method (TLLBM) [13]. When the TLLBM technique is applied to eq. (5), the final form is:

$$f_i(x, t \quad \delta t) \quad \sum_{k \;\; 1}^{M \;\; 1} a_{1k} \, \overline{f}_{k \;\; 1} \tag{15}$$

where a_{1k} are the elements of the first row of the matrix [A] defined as:

$$A([S]^{\mathrm{t}}[S])^{-1}[S]^{\mathrm{t}}$$

$$[S] = \begin{matrix} 1 & \Delta x_{\mathrm{A}} & \Delta y_{\mathrm{A}} & \frac{(\Delta x_{\mathrm{A}})^2}{2} & \frac{(\Delta y_{\mathrm{A}})^2}{2} & \Delta x_{\mathrm{A}} \Delta y_{\mathrm{A}} \\ 1 & \Delta x_{\mathrm{B}} & \Delta y_{\mathrm{B}} & \frac{(\Delta x_{\mathrm{B}})^2}{2} & \frac{(\Delta y_{\mathrm{B}})^2}{2} & \Delta x_{\mathrm{B}} \Delta y_{\mathrm{A}} \\ - & - & - & - & - & - \\ - & - & - & - & - & - \\ - & - & - & - & - & - \\ 1 & \Delta x_{\mathrm{M}} & \Delta y_{\mathrm{M}} & \frac{(\Delta x_{\mathrm{M}})^2}{2} & \frac{(\Delta y_{\mathrm{M}})^2}{2} & \Delta x_{\mathrm{M}} \Delta y_{\mathrm{M}} \end{matrix} \tag{16}$$

where $x_{\mathrm{M}} = x_{\mathrm{M}} + c_{\mathrm{ix}} \delta t - x_{\mathrm{p}}$, $y_{\mathrm{M}} = y_{\mathrm{M}} + c_{\mathrm{iy}} \delta t - y_{\mathrm{P}}$, and

$$\overline{f}_{k} \quad 1 \quad \frac{1}{\tau} \; f_i(\vec{\mathrm{x}}, \vec{\mathrm{c}}_i, t) \quad \frac{1}{\tau} f_i^{eq}(\vec{\mathrm{x}}, \vec{\mathrm{c}}_i, t) \tag{17}$$

The temperature field by FV method

The numerical approach used to solve the energy equation is based on a classical FV approximation [14]. Let consider a two-dimensional convection – diffusion equation for a general variable φ coupled to the continuity equation:

$$\frac{\partial \varphi}{\partial t} \qquad [F(\varphi)] \quad f \tag{18}$$

in which $F(\varphi) = \vec{\mathrm{u}}\varphi \quad \gamma_\varphi \quad \varphi$ is the advection-diffusion tensor with the convective part $Fc = \vec{\mathrm{u}}\varphi$ and the diffusive part $Fd = \gamma_\varphi \quad \varphi$.

Equation (18) gives the expression of the conservation of the variable φ in an infinitesimal domain, it can be written in any sub-domain V and for all time t and t' as:

$$\int_V \varphi(\vec{x}, t)\,dx \int_V \varphi(\vec{x}, t)\,d\vec{x} \int_t^{t} \int_{\partial V} F\tau_V(\vec{x})\,d\sigma(\vec{x})\,d\vec{x}\,dt \int_V^{t} \int_t f(\vec{x}, t)\,d\vec{x}\,dt \tag{19}$$

where $\tau_V(x)$ is the normal vector to the boundary V at point x, outward to V.

In order to define a FV scheme, the time derivative is approximated by a finite difference scheme on an increasing sequence on time $(t_n)n \in \mathrm{IN}$ with $t_0 = 0$. The discrete unknowns at time $t_n = n\delta t$, are expected to be an approximation of φ around the point M_{ij} on the cell V and noted φ_{ij}^n.

Equation (14) is integrated over each cell V using the Gauss divergence theorem (fig. 2):

$$\int_V \frac{\partial \varphi}{\partial t}^{n} dx \int_{\partial V} F^{n}\vec{\tau}_V\,d\sigma(\vec{x})\,dx \int_V f(\vec{x}, t_n)\,d\vec{x} \tag{20}$$

where $(\partial\varphi/\partial t)^n$ is given by the time scheme at the time step $t_n = n\,\delta t$ in the control volume V. The next step of the method is the approximation of the convective part $F_c \cdot \tau_V$ and the diffusive part $F_d \cdot \tau_V$ of the projected flux $F \cdot \tau_V$ over the boundary ∂V of each control volume.

The time integration is performed implicitly by using a three level Euler scheme, given a second order truncation error in time.

The diffusive part of the flux is discretized with a second order truncation error in space (if uniform mesh). Different discretizations for the convective fluxes are possible, central schemes apply a symmetric interpolation for $\varphi_{i+1/2}$. Upwind schemes apply a one side interpolation. Leonard [15-16] has introduced Quick and other schemes as a combination between the two kinds of interpolation. We have used the Quick scheme with a second order truncation in space. Verifications and validations are achieved and detailed in [25].

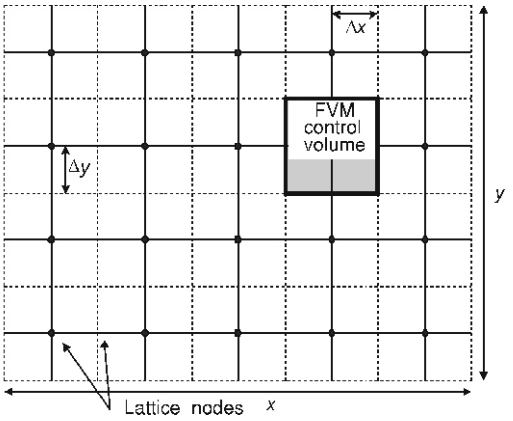

Figure 2. Lattice nodes and control volumes in a 2-D rectangular geometry

The good stability properties of the scheme have been exhibited for time-dependent Navier-Stokes equations for fluid flow and extended to phase change configuration exhibiting strong solid/liquid interactions.

Phase change treatment

As mentioned before, in a phase change system of a pure metal, three distinct regions will be present (fig. 3): a full solid zone (heat transfers), a full liquid zone (dynamic), and a solid-liquid interface region. In this study a mathematical model is developed to study the phase change problems and using any phase change material. Liquid phase is Newtonian and incompressible, the flow is laminar; it is further assumed that the third dimension of the cav-

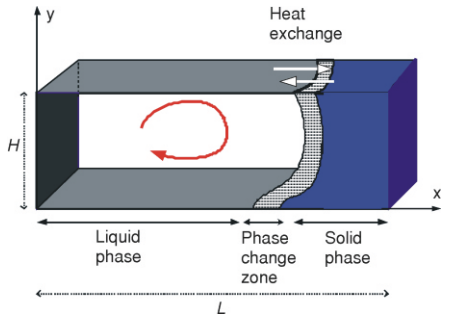

Figure 3. Illustration of transfers in the horizontal Bridgman cavity

ity is sufficiently long to consider the flow two-dimensional. Viscous dissipation is negligible in comparison with conduction and convection.

An enthalpy formulation is used (eq. 3) by considering continuum media for thermal field [17-18]. The melting process takes place over a temperature range $T_f \quad \varepsilon$ where ε is a small quantity (typically $\varepsilon = 5\%$ of ΔT). The basic idea of the enthalpy method is to separate the sensible and latent heat components in the vicinity of the solid-liquid interface ($T_f - \varepsilon \quad T \quad T_f + \varepsilon$). The latent heat component is expressed in term of the latent heat L_f and liquid fraction ϕ, which is defined as:

$$\begin{aligned} \phi \quad & 1 && \text{for} \quad T \quad T_f \quad \varepsilon \\ \phi \quad & 0 && \text{for} \quad T \quad T_f \quad \varepsilon \\ \phi \quad & \frac{(T \quad T_f \quad \varepsilon)}{2\varepsilon} && \text{for} \quad T_f \quad \varepsilon \quad T \quad T_f \quad \varepsilon \end{aligned} \tag{21}$$

Dynamically, the solid/liquid interface is treated like a boundary condition. In practice, the boundary conditions are given according to the macroscopic variables $\vec{u}$ and ρ. However, in the LB method, the real boundary conditions must be transformed into relations on the distribution functions at each lattice point of the boundaries. The choice of these relations can affect the accuracy and the stability of the method [1-2]. For the LB method, at the boundaries, the particle distribution functions f_i going inside the medium are unknown and there are computed from the boundary conditions and f_i going outside the medium.

In the present study, the solid/liquid interface is treated like a curved solid boundary conditions (BC). For this kind of BC, several schemes were developed. We adopted the extrapolation proposed by Bao *et al.* [18]. In fig. 2, the curved interface is located between solid node and fluid node, with $\Delta = |x_f \quad x_w| / |x_f \quad x_b|$ denoting the fraction of link of the fluid zone. The volume surrounding the lattice node x_b is not homogeneous and contains both the solid and liquid phases. The streaming step is treated differently by computing $\tilde{f}_{\bar{i}}(x_f, t)$ at boundary node x_b, where $\tilde{f}_{\bar{i}}$ is the post-collision state of the distribution function. As it is proposed by Filippova *et al*. [19] and revised by Mei *et al.* [20], the following relations on the curved interface are used:

$$\tilde{f}_{\bar{i}}(\vec{x}_b, t) \quad (1 \quad \chi)\tilde{f}_{\bar{i}}(\vec{x}_f, t) \quad \chi f_i^*(\vec{x}_f, t) \tag{22}$$

where χ is the weighting factor.

To guarantee the mass conservation, $f_i^*(x_b, t)$ is defined by:

$$f_i^*(x_b, t) \quad \omega_i \rho(x_w, t)\, 1 \quad 3\frac{\vec{e}_i \quad \vec{u}_{bf}}{c^2} \quad \frac{9}{2}\frac{(e_i \quad \vec{u}_f)^2}{c^4} \quad \frac{3}{2}\frac{\vec{u}_f \quad \vec{u}_f}{c^4} \tag{23}$$

where $\rho(x_w, t)$ is called the wall density; it is computed so as to ensure not loss of the mass at the solid boundary. $\vec{u}_{bf}$, χ, and $\rho(x_w, t)$ are given by:

$$\vec{u}_{bf} \quad \vec{u}_f \quad \frac{3}{2\Delta}\vec{u}_f \quad \text{and} \quad \chi \quad \frac{2\Delta \quad 1}{\tau \quad \frac{1}{2}} \quad \text{for} \quad \Delta \quad \frac{1}{2} \tag{24}$$

$$\vec{u}_{bf} \quad \vec{u}_{ff} \quad \text{and} \quad \chi \quad \frac{2\Delta \quad 1}{\tau \quad 2} \quad \text{for} \quad \Delta \quad \frac{1}{2} \tag{25}$$

$\rho(x_w, t)$ is calculated from the conservation mass relation:

$$\sum_{\text{autcoming}} f_i \qquad \sum_{\text{incoming}} f_i$$

The use of the present implementation of the mass conserving BC makes it possible precisely take account of the convection interaction with the form and the progression of the solid-liquid interface (fig. 4). This technique returns the method of tracked interface dynamically possible in LB method.

Benchmarking

First, it is important to mention that the pure convective solution is in good agreement with the traditional exercise of a cavity differentially heated containing a fluid with air Prandtl (Pr = 0.71). The Rayleigh number is varied between Ra = 10^3 and Ra = 10^6. The numerical values are in good agreement with the reference results [21] (see tab. 1). The present method thus exhibits good aptitudes to simulate accurately thermoconvectives phenomena. The following work focus on the phase change coupling.

In the case of phase change occurrence, the authors adopted a methodology of validation by considering first a classical phase change Stefan problem followed by a situation of phase change coupling conductive and convective transfers.

Table 1. Results of the convection test in a differentially heated square cavity (present values – bold, de Vahl Davis results [21])

Ra	u_{max}		v_{max}	
10^3	**3.699**	3.697	**3.650**	3.649
10^4	**19.620**	19.617	**16.213**	16.178
10^5	**68.68**	68.59	**34.817**	34.73
10^6	**220.418**	219.36	**64.763**	64.63

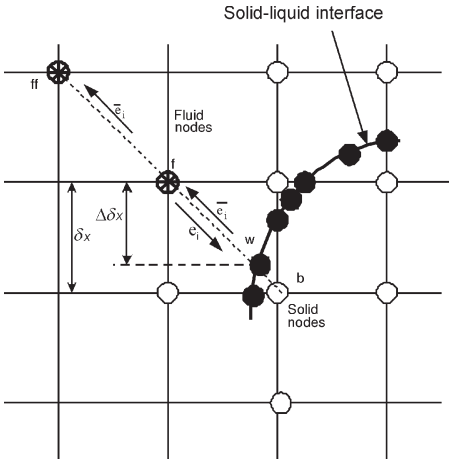

Figure 4. Lay-out of the lattice and curved solid-liquid interface

Benchmark 1: LBFVM vs. heat-balance integral method (HBIM) for Stefan problem

This exercise aims to evaluate the ability of the method to treat the phase change problem in the condition of a pure diffusion. 1-D solidification systems (the called Neumann problem) is considered [22]. The geometry configuration and the boundary conditions are shown in fig. 5.

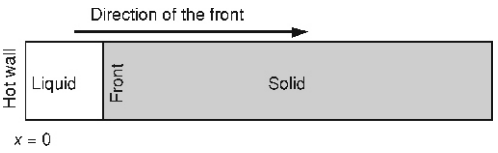

Figure 5. Sketch of the geometry and boundary conditions for the Stefan problem

A liquid at a uniform temperature T_H that is at or higher than the melting temperature T_m of the solid phase is confined to a half-space $x > 0$. At time $t = 0$ the boundary surface at $x = 0$ is lowered to a temperature T_C below T_m and maintained at that temperature for times $t > 0$. As a result, solidification starts at the surface $x = 0$ and the solid-liquid interface moves in the positive x-direction.

An analytical solution of the location of the solidification interface in the semi-infinite domain is given by the relation:

$$X(t) \quad 2\lambda\sqrt{\alpha t} \tag{26}$$

where α is the coefficient of heat diffusion and λ – a constant controlled by the following algebraic equation:

$$\frac{\mathrm{Ste}}{\sqrt{\pi}} \quad \lambda \mathrm{e}^{\lambda^2} \quad \frac{1}{\mathrm{erf}(\lambda)} \quad \frac{\theta_{\mathrm{F}}}{\mathrm{erfc}(\lambda)}^{1} \tag{25}$$

Simulations were carried out in a rectangular cavity of aspect ratio 0.04 of the domain and a Stefan number of Ste = 0.5. Table 2 shows a good agreement between our work and HBIM simulation. Figure 6 shows a good agreement of the numerical results (LBFVM) with the analytical estimations for a value $\lambda = 0.445$. The error introduced by the consideration of a finite domain remains negligible for the positions of the interface not exceeding a maximum limit. This validation shows the capacity of the method to describe accurately the progression of the solid-liquid interface in a conductive mode.

Table 2. Comparison of the present solution with HBIM method for different values of Ste

Ste	λ^{LBFVM}	λ^{HBIM}
0.01	0.0706	0.0707
0.1	0.2228	0.2232
1	0.6589	0.6600
10	1.2723	1.2903
100	1.7260	1.5991

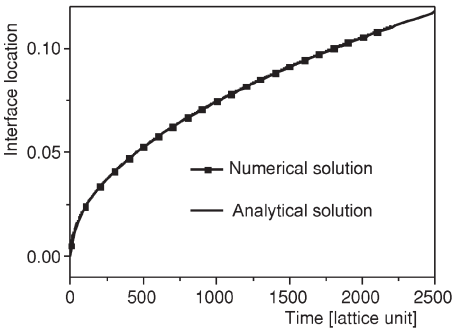

Figure 6. Numerical and analytical melting front location for 1-D Stefan problem (Ste = 0.5)

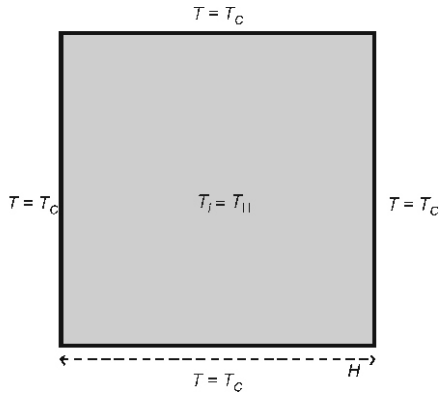

Figure 7. Geometry and boundary conditions of the solidification case

Benchmark 2: solidification interacting with fluid flow

This exercise is devoted to the interaction of the convection with the solidification occurrence. A thermal shock held on the liquid surface (presenting an analytical solution in the conductive case, *i. e.* Ra = 0). The domain presented in fig. 7 is a square cavity filled with a liquid phase (characterized by a Prandtl number Pr = 7.36) and brought up to an dimensionless hot temperature ($T_{\mathrm{H}} = 0.33$). Brutally, we applied a cold temperature ($T_{\mathrm{C}} = -0.67$) at the edges. The dimensionless melting temperature is $T_{\mathrm{m}} = 0$.

The semi-analytical of this problem, for Ra = 0, in a semi infinite region was obtained by Rathjen *et al.* [23]. The numerical results in the diffusive regime are in good agreement with

the analytical solution. The study of Rathjen *et al*. solution is extended here to convective regimes.

The set of eqs. (1)-(3) is solved for dimensionless numbers: Ra = $g\beta\Delta TH^3/\nu\alpha$ [0.10^8], Ste = $Cp\Delta T/L_f$ [0.1, 1.0], and Pr = 7.36. The domain consists on a rectangular cavity (fig. 7). The boundary and initial conditions are given as:

– initial conditions

$$x \quad \Omega \quad [0,1] \quad [0,1], \quad T\big|_{t\ 0} \quad 1, \quad \vec{u}\big|_{t\ 0} \quad 0$$

– boundary conditions

$$T\big|_{x\ \partial\Omega} \quad 1, \quad \vec{u}\big|_{x\ \partial\Omega} \quad 0$$

Results presented here are gotten with $Nx \times Ny = 100 \times 100$ for and 200×200 for Ra = 10^8. More accurate results can be obtained through calculations with a finer mesh, but they require more computer CPU time and memory capacity. Therefore, a non-uniform mesh is adopted in order to save CPU time while maintaining accuracy. The grid points are distributed as small grid spacing near the left wall to obtain sufficient resolution of the boundary layers formed along the surfaces.

The phase change phenomenon (solidification) of the fluid was studied for various Rayleigh numbers. For Ra 10^6, the convective motion intensity is very weak and do not affect the kinetics of the phase change. This is well illustrated in fig. 8. Indeed, because of the fluid flow developed in the melt zone, the maximum temperature falls rapidly, which is not the case for low Ra. This conclusion is valid for the evolution of the liquid fraction which tends quickly towards 0 for high Ra. The convective motion developed within the fluid zone improves heat transfer between the two phases and accelerate consequently the solidification process for high Ra.

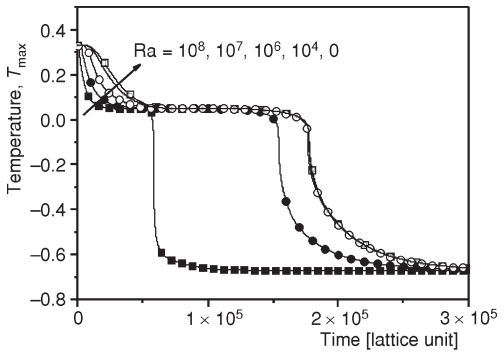

Figure 8. Evolution of the maximum temperature (Ste = 0.5)

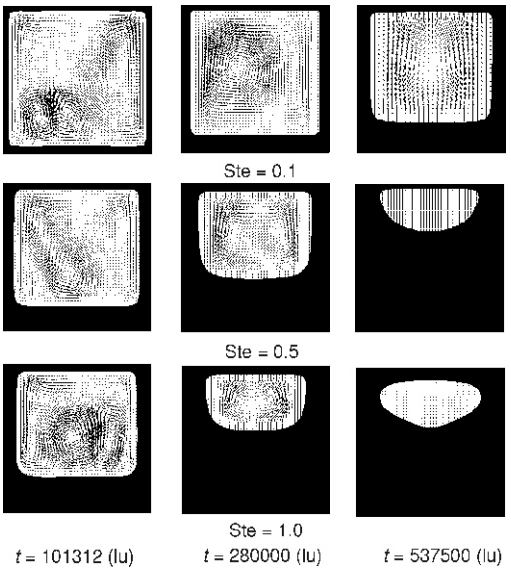

Figure 9. Interfaces and velocity at different instants of solidification for various Stefan numbers (Ra = 10^8) (lu – lattice unit)

Also the latent heat effect (Stefan number) on the convective cells is studied. This effect is simulated for the Rayleigh number value (Ra = 10^8). Figure 9 shows the velocity field progression and the behavior of the solid-liquid interface. For Ste = 0.1 and Ste = 0.5, the latent heat is very important, this delays the progression of the solid-liquid interface (fig. 10). This situation is in favor of the development and the intensification of the convective move-

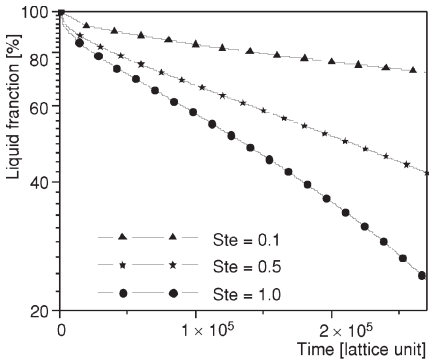

Figure 10. Evolution of the total liquid fraction for various Stefan numbers for Ra = 10^8

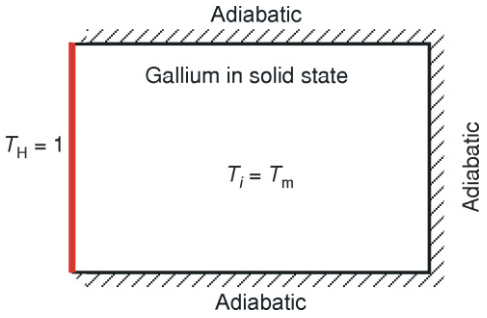

Figure 11. Geometry and boundary conditions of the melting case

ments and consequently, a significant effect on the progression and the form of the solid-liquid interface can be noted. This effect is less significant in the case of Ste = 1.

Benchmark 3: melting interacting with fluid flow

The experimental analysis of the melting of the gallium in a rectangular cavity from a vertical wall was initially proposed by Gau *et al.* [9]. A particular attention has been carried on the buoyancy-induced flow in the pure metal and its effect on the solid-liquid interface position and heat transfer conditions. This experience has been considered as a test case to qualify the mathematical formulations used for the numerical simulation of phase change problems since first numerical results of Brent *et al.* [24] using an enthalpy-porosity formulation FV solved at first order [9]. Semma *et al.* showed how the accuracy of the used scheme affects directly the multicellular flow occurrence [25]. The Gallium is contained in a two-dimensional rectangular cavity of height H and width L (fig. 11). The material is assumed to be initially in solid state at its melting temperature T_m = 28.3 °C. The temperature at the bottom surface is increased suddenly to 38.0 °C, while the other walls are maintained in adiabatic state. At time $t = 0$, the temperature of the left vertical wall is raised impulsively to a prescribed temperature above the fusion point, $T_w > T_m$.

The set of equations (1)-(3) is solved for dimensionless numbers corresponding to experimental data of Gau *et al.* [9]: Ra = $g\beta\Delta TH^3/\nu\alpha$ 7·105, Ste = $Cp\Delta T/L_f$. The domain consists on a rectangular cavity. The boundary and initial conditions are given as follows:

– initial conditions

$$x \quad \Omega \quad [0,1.43] \quad [0,1], \quad T\big|_{t\ 0} \quad 1, \quad \vec{u}\big|_{t\ 0} \quad 0$$

– boundary conditions

$$\left.\frac{\partial T}{\partial n}\right|_{x\ A;y\ 0;y\ 1} \quad 0, \quad T\big|_{x\ 0} \quad 1, \quad \vec{u}\big|_{x\ \partial\Omega} \quad 0$$

Results presented here are gotten with $Nx \times Ny = 201 \times 140$. More accurate results can be obtained through calculations with a finer mesh, but they require more CPU time. Therefore, a non-uniform mesh is adopted in order to save CPU time while maintaining accuracy. The grid points are distributed as small grid spacing near the left wall to obtain sufficient resolution of the boundary layers formed along the surfaces.

The evolution of melting front is compared with those measured by Gau *et al.* [9] as shown in fig. 12. The interface position given by the present enthalpy model is in good agreement with the reference results. The initial temperature and the difficulty to maintain a constant

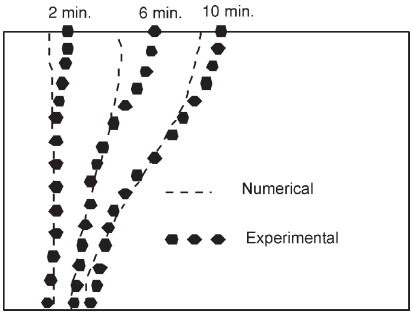

Figure 12. Numerical and experimental solid-liquid interface profiles

temperature on the heated wall can be a source of discrepancies between the predicted solid/liquid front and the experimental one.

The numerical results in terms of flow structures and solid-liquid interface position are in good agreement with reference results [26-28]. Indeed, at the beginning of fusion process, there is appearance of a one flow cell with low intensity for ($t < 20$ s). Thereafter and with the progression of the interface and the increase of the Rayleigh number of the liquid zone, there is bifurcation towards a multi cellular structure. When the melt size increases with time, the number of flow cells decreases by merging of the two upper cells.

Conclusions

A methodology coupling lattice Boltzman and finite volume approaches is developed for modelling solid-liquid phase change problems.

Benchmarking have been operated for conductive and convective solution exhibiting analytical solution or experimental results and present numerical results are in good agreement with and show the ability of the high-order finite volume coupled to lattice Boltzmann method to solve stiff phase change problems.

One important extension is the possible use of such coupling to study complex configurations of crystal growth associating the efficiency of the finite volume approach for conservative laws and the flexibility of the lattice Boltzman approach for complex geometries.

References

[1] Bouzidi, M., Firdaouss, M., Lallemand, P., Momentum Transfer of a Boltzmann-Lattice Fluid with Boundaries, *Phys. Fluids, 13* (2001), 11, pp. 3452-3459
[2] Chen, S., Doolen, G., Lattice Boltzmann Method for Fluid Flows, *Annual Review of Fluid Mechanics,* Annual Reviews, Palo Alto, Cal., USA*, 30* (1998), January, pp. 329-364
[3] Ginzburg, I., Steiner, K., A Free-Surface Lattice Boltzmann Method for Modelling the Filling of Expanding Cavities by Bingham Fluids, *Phil. Trans. R. Soc. Lond. A, 360* (2002), March, pp. 453-466
[4] Alexander, F. J., Chen, S., Sterling, J. D., Lattice Boltzmann Thermohydrodynamics, *Physical Review E, 47* (1993), 4, pp. R2249-R2252
[5] Bhatnagar, P., Gross, E., Krook, M., A Model for Collision Process in Gases, I: Small Amplitude Processes in Charged and Neutral One-Component Systems, *Phys. Rev. E, 94* (1954), 3, pp. 511-525
[6] Chen, S., Doolen, G., Lattice Boltzmann Method for Fluid Flows, *Annual Review of Fluid Mechanics,* Annual Reviews, Palo Alto, Cal., USA, *30* (1998), January, pp. 329-364
[7] Ginzburg, I., Steiner, K., A Free-Surface Lattice Boltzmann Method for Modelling the Filling of Expanding Cavities by Bingham Fluids, *Phil. Trans. R. Soc. Lond. A, 360* (2002), March, pp. 453-466
[8] Ganaoui, M. El, *et al*., Computational Solution for Fluid Flow under Solid/Liquid Phase Change Conditions, *Int. J. Computers and Fluids, 31* (2002), 4-7, pp. 539-556
[9] Gau, C., Viskanta, R., Melting and Solidification of a Metal System in a Rectangular Cavity, *Int. J. Heat Mass Transfer, 27* (1984), 1, pp. 113-123
[10] Frisch, U., Hasslacher, B., Pomeau, Y., Lattice Gas Automata for the Navier Stokes Equation, *Phys. Rev. Lett., 56* (1986), 14, pp. 1505-1508
[11] Bhatnagar, P., Gross, E., Krook, M., A Model for Collision Process in Gases, I: Small Amplitude Processes in Charged and Neutral One-Component Systems, *Phys. Rev. E, 94* (1954), 3, pp. 511-525
[12] Hou, S., *et al.*, Simulation of Cavity Flow by the Lattice Boltzmann Method, *J. Comput. Phys., 118* (1995), 2, pp. 329-347

[13] Shu, C., Peng, Y., Chew,Y. T., Simulation of Natural Convection in a Square Cavity by Taylor Series Expansion and Least Squares-Based Lattice Boltzmann Method, *International Journal of Modern Physics C, 13* (2002), 10, pp. 1399-1414
[14] Peyret, R., Taylor, T. D., Computational Methods for Fluid Flow, Springer-Verlag, New York, USA, 1983
[15] Mohamad, A. A., Applied Lattice Boltzmann Method for Transport Phenomena, Momentum, Heat and Mass Transfer, Sure Printing, Calgary, Alberta, Canada, 2007
[16] Leonard, B. P., Mokhtari, S., Beyond First Order Upwinding: The ULTRA-SHARP Alternative for Non-Oscillatory Steady-State Simulation of Convection, *Int. J. Numerical Methods Eng, 30* (1990), 4, pp. 729-766
[17] Semma, E. A., El Ganaoui, M., Bennacer, R., Lattice Boltzmann for Melting/Solidification Problems, *Comptes Rendus Mécanique, 335* (2007), 5-6, pp. 295-303
[18] Semma, E. A., El Ganaoui, M., Bennacer, R., Mohamad, A. A., Investigation of Fows in Solidifcation by Using the Lattice Boltzmann Method, *International Journal of Thermal Sciences, 47* (2008), 3, pp. 201-208
[19] Filippova, O., Hänel, D., Grid Refinement for Lattice – BGK Models, *J. Comp. Phys., 147* (1998), 1, pp. 219-228
[20] Mei, R., Luo, L-S., Shyy, W., An Accurate Curved Boundary Treatment in the Lattice Boltzmann Method, *J. Comp. Phys, 155* (1999), 2, pp. 307-329
[21] de Vahl Davis, G., Natural Convection of Air in a Square Cavity: A Benchmark Numerical Solution, *Int. J. Numerical Methods in Fluids, 3* (1983), 3, pp. 249-264
[22] Ozisik, M. N., Heat Conduction, John Wiley and Sons, New York, USA, 1980
[23] Rathjen, K.A., Jiji, L. M., Heat Conduction with Melting or Freezing in a Corner, *J. Heat Transfer, 93* (1971), 1, pp. 101-109
[24] Brent, A. D., Voller, V. R., Reid, K., The Enthalpy-Porosity Technique for Modeling Convection-Diffusion Phase Change: Application to the Melting of a Pure Metal, *J. Num. Heat Transfer B, 13* (1988), 3, pp. 297-318
[25] Semma, E. A., *et al*., High Order Finite Volume Scheme for Phase Change Problems. Finite Volumes for Complex Applications IV (Eds. F. Benkhaldoun, D. Ouazar, S. Raghay), Hermés Science Publishing Ltd., London, 2005, pp. 493-503
[26] Stella, F., Giangi, M., Melting of a Pure Metal on a Vertical Wall: Numerical Simulation, *Numerical Heat Transfer A, 38* (2000), 2, pp. 193-208
[27] Campbell, T. A., Koster, J. N., Visualization of Liquid-Solid Interface Morphologies in Gallium Subject to Natural Convection, *J. Crystal Growth, 140* (1994), 3-4, pp. 414-425
[28] Lacroix, M., Voller, V. R., Finite Difference Solutions of Solidification Phase Change Problems: Transformed Versus Fixed Grids, *Numerical Heat Transfer B, 17* (1990), 1, pp. 25-41

Authors´ affiliations:

M. El Ganaoui (**corresponding author**)
Université de Limoges/CNRS,
SPCTS UMR 6638, 123 Albert Thomas,
87000 Limoges, France
E-mail: ganaoui@unilim.fr

E. A. Semma
Laboratoire de Mécanique (LM),
Faculté des Sciences et Techniques de Settat,
Settat, Maroc

Paper submitted: September 9, 2008
Paper revised: February 17, 2008
Paper accepted: February 26, 2008